# The calculated electronic and magnetic structures of Fe4N and Mn 4N

Samir F. Matar, P. Mohn, Gérard Demazeau, B. Siberchicot

*J. Phys. France* **49** (1988) 1761-1768 OCTOBRE **1988,** PAGE 1761

Classification
*Physics Abstracts*
71.20

# The calculated electronic and magnetic structures of $Fe_4N$ and $Mn_4N$

S. Matar, P. Mohn (*), G. Demazeau and B. Siberchicot

Laboratoire de Chimie du Solide du CNRS, Université de Bordeaux I, 351 cours de la Libération, 33405 Talence Cedex, France

(*Reçu le 29 avril 1988, révisé le 9 juin 1988, accepté le 20 juin 1988*)

**Résumé.** — Utilisant la méthode de l'« onde sphérique augmentée » (augmented spherical wave) les auteurs ont calculé les structures électroniques et magnétiques de $Fe_4N$ et de $Mn_4N$. Les deux nitrures s'ordonnent magnétiquement avec un alignement ferro- et ferri-magnétique respectivement. Les valeurs obtenues des moments magnétiques sont en bon accord avec celles de la littérature. Une comparaison avec le modèle phénoménologique de Goodenough ainsi qu'avec les alliages de Heusler est donnée.

**Abstract.** — Using the augmented spherical wave method (A.S.W.) we calculate the electronic and magnetic structures of $Fe_4N$ and $Mn_4N$. Both nitrides are found to order magnetically exhibiting ferro- and ferrimagnetic spin alignment respectively. The magnetic moments found are in good agreement with neutron data. Both systems can be described *via* covalent magnetism. A comparison with Goodenough's phenomenological model as well as with Heusler alloys is given.

## 1. Introduction.

Recent investigations on $Fe_4N$ as a recording material by Suzuki *et al.* [1], Tagawa *et al.* [2] and Demazeau *et al.* [3] started a renaissance of the first row of the transition-metal nitrides. This class of compounds was subject to intensive experimental and theoretical studies in the late fifties and early sixties [4-7] and with less interest since. $Fe_4N$ and derived « carbo-nitrides » (of formulation $Fe_4N_{1-\varepsilon}C_\varepsilon$ with $\varepsilon \simeq 0.3$) are now being investigated among most promising magnetic pigments for high density recording [8].

The crystal structure of $Fe_4N$ is shown in figure 1a. It can be visualized as an f.c.c. iron lattice with an additional nitrogen atom at the center of the cell. Whereas one iron (sub)lattice is observed in f.c.c. Fe (space group Fm3m), two iron sublattices can be accounted for in $Fe_4N$ (space group Pm3m) :

(i) the Fe atoms at the cube corner positions (hereafter referred to as Fe(I)) ;

(ii) the Fe atoms at the face center positions (hereafter referred to as Fe(II)).

(*) Technische Universität Wien, Getreidemarkt 9/158 ; 1-1060, Wien, Austria.

The insertion of nitrogen leads to an expansion of the cell-volume of an f.c.c. Fe-type lattice ($\gamma$-Fe). The lattice constant of $Fe_4N$ accurately determined to 3.797 Å [4] is 10 % larger than that of $\gamma$-Fe ($a$ = 3.450 Å). The crystallographic position of N

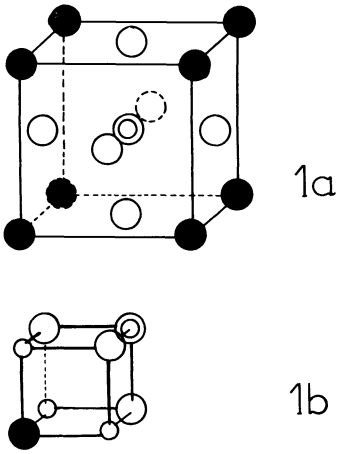


Fig. 1. — (a) The crystal structure of $M_4N$ (M = Fe, Mn) ; (b) location of the empty sphere in the $M_4N$ structure (Full circles : M(I) ; open circles : M(II) ; double circles : N and small open circles : empty spheres.)

leads to 6 Fe(II)-N distances shorter than 8 Fe(I)-N ones ($d$(6 Fe(II)-N) $\simeq$ 1.90 Å ; $d$(8 Fe(I)-N) $\simeq$ 3.29 Å). These geometrical considerations suggest that iron-nitrogen interactions would preferentially occur between face-center iron atoms and central nitrogen rather than between corner iron atoms and nitrogen.

Such a phenomenological description of the chemical bond in $Fe_4N$ — as well as in other transition metal nitrides — needs, in our view, further support by using band calculation methods for the electronic structure of solids.

The present investigation on $Fe_4N$ will be carried out along with isostructural $Mn_4N$, a ferrimagnetic nitride thouroughly investigated by Fruchart *et al.* [9].

## 2. Method of calculation.

The electronic structures of both $Fe_4N$ and $Mn_4N$ were calculated employing the ASW (Augmented Spherical Wave) method [10]. These self-consistent *ab initio* calculations are based on the local spin density functional treatment of exchange and correlation by V. Barth and Hedin [11] and Janak [12]. The Brillouin-zone integration was carried out for 10 independent $k$-points on a uniform mesh in the irreducible wedge. This limited number of $k$ points insured accurate results with minimum computing expenses ; however a larger number of $k$ points could improve the reliability of the values of the magnetic moments. The matrix elements were constructed involving solutions of the Schrödinger equation up to $l + 1$ where $l = 2$ for the transition metal and $l = 1$ for nitrogen. The contribution associated with the $l + 1$ term includes corrections due to internal summation over the three-center terms. The self consistency cycle was carried out until energy convergence on a scale better than 1 mRyd was achieved.

We chose the ASW-method firstly because of its merit describing metallic systems and systems involving covalent interactions [13-15] and secondly because of its efficiency in terms of computer time, as a linearized method.

## 3. Calculations and results.

The structure of $Fe_4N$ — and $Mn_4N$ — is a rather poorly packed one — contrary to f.c.c. or h.c.p. ones —. This induced us to introduce empty spheres — pseudo-atoms with $Z = 0$ — in the manner shown in figure 1b. These empty spheres contain the « tails » of the spherical wave functions — predominantly Fe —. On the other hand such empty spheres would account for possible covalency effects [14].

Fully self-consistent « spin-polarized » — i.e. for magnetically-ordered structures — band calculations have been performed for both nitrides. Self consistency was achieved after 30 iterations. The local partial charges are given in table I. In both cases there is hardly any charge transfer between nitrogen and any of the metallic atoms. Inasfar as 2s and 2p are considered as valence states for N — actually N-2s is in a semi-core state —, the charge remains close to 5 : 4.98 and 5.00 for $Fe_4N$ and $Mn_4N$ respectively. This finding rules out any support for an ionic model for nitrogen in such compounds as proposed in the early literature [16]. We find, however, a strong overlap between the N-2p and the lower d-states of Fe(II) hence suggesting a covalent bond between these atoms.

There is hardly any interaction between N and Fe(I). Both Fe(I) and Fe(II) loose electrons to the

Table I. — *Local partial charges for spin up* (↑) *and spin down* (↓) *directions for* $Fe_4N$ *and* $Mn_4N$ *(the values between brackets are residues corresponding to higher* 1*-term charges).*

| | | $n_s$ ↑ | $n_s$ ↓ | $n_p$ ↑ | $n_p$ ↓ | $n_d$ ↑ | $n_d$ ↓ | $n_f$ ↑ | $n_f$ ↓ | $M(\mu_B)$ | Experiment |
|---|---|---|---|---|---|---|---|---|---|---|---|
| $Fe_4N$ | Fe(I) | 0.20 | 0.20 | 0.18 | 0.20 | 4.58 | 1.58 | (0.01) | (0.01) | 2.98 | 3.00 (*) |
| | Fe(II) | 0.21 | 0.21 | 0.27 | 0.29 | 4.12 | 2.31 | (0.04) | (0.04) | 1.79 | 2.00 (*) |
| | N | 0.72 | 0.72 | 1.72 | 1.72 | (0.06) | (0.04) | | | 0.02 | |
| | $E_s$ | 0.24 | 0.28 | 0.14 | 0.12 | (0.05) | (0.03) | | | 0.00 | |
| $Mn_4N$ | Mn(I) | 0.18 | 0.22 | 0.18 | 0.23 | 0.96 | 4.11 | (0.01) | (0.01) | − 3.23 | + 3.85 (**) |
| | Mn(II) | 0.20 | 0.20 | 0.28 | 0.28 | 3.10 | 2.31 | (0.04) | (0.04) | 0.80 | − 0.90 (**) |
| | N | 0.71 | 0.72 | 1.69 | 1.78 | (0.06) | (0.04) | | | − 0.07 | |
| | $E_s$ | 0.27 | 0.28 | 0.14 | 0.15 | (0.04) | (0.04) | | | − 0.02 | |

$E_s$ = empty sphere.
(*) Frazer B. C. [4].
(**) Takei W. J. *et al.* [24].

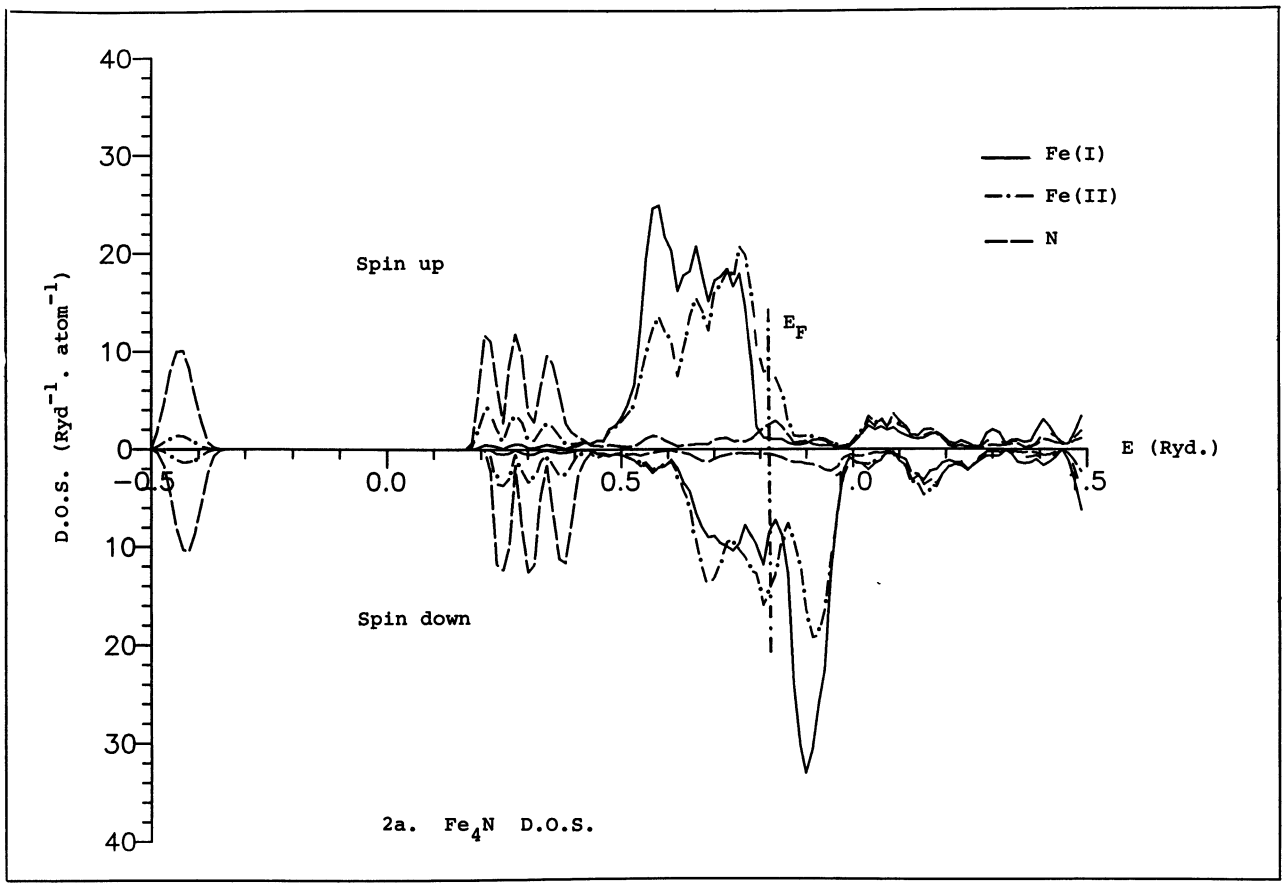


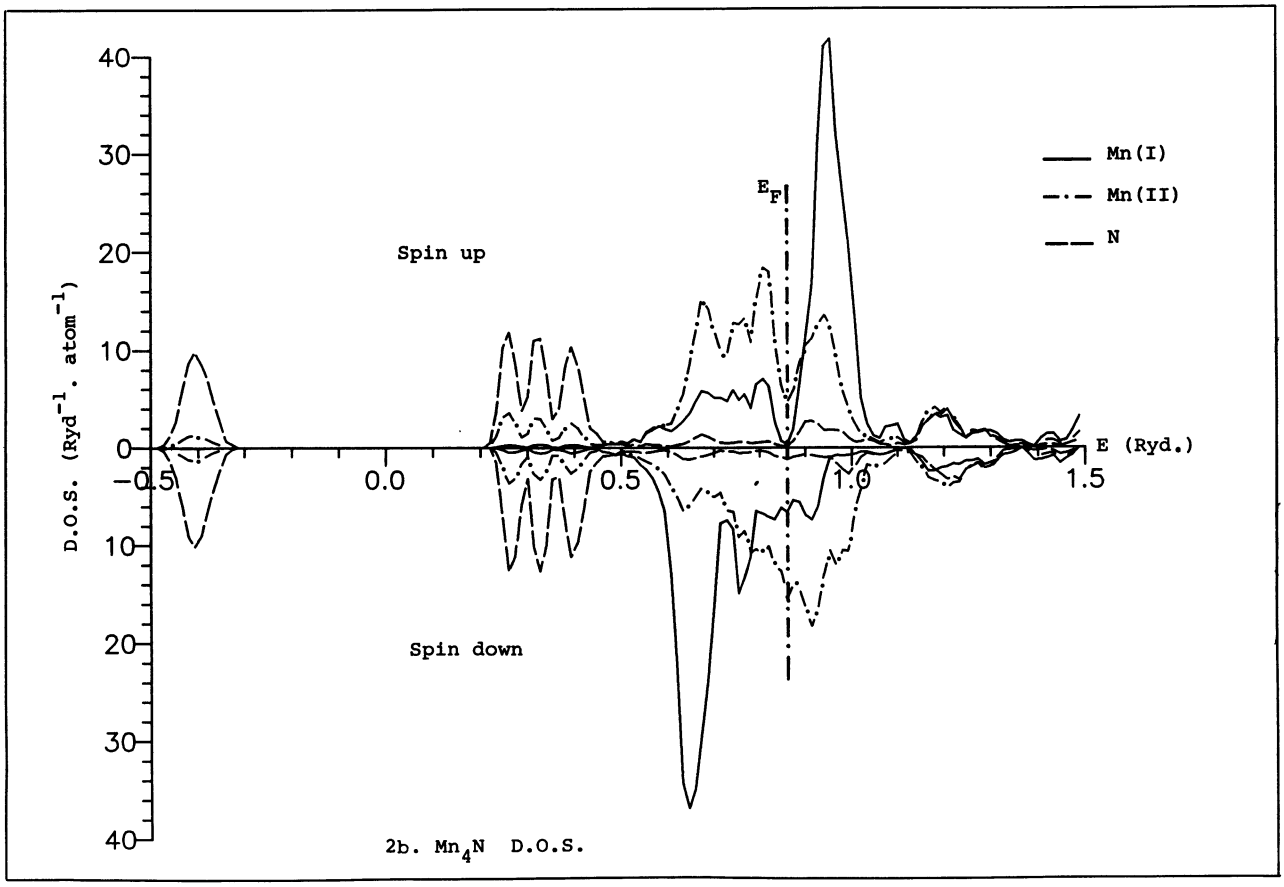


Fig. 2. — Site and spin projected D.O.S. for : (a) $Fe_4N$ ; (b) $Mn_4N$.

empty spheres but the main contribution of the charge inside these spheres is supplied by the Fe(I) atoms : their t2g states interact with those of Fe(II) forming bonding and anti-bonding d-d states. The energetically low-lying eg states remain localized and point in the direction of the empty sphere thus transferring charge into it.

Figures 2a and 2b show the site and spin-projected densities of states (D.O.S.) for $Fe_4N$ and $Mn_4N$. The localized eg states can be clearly seen at the bottom and top of the d-band. For Fe(II) and Mn(II) these states are broadened by the interaction with N-2p states.

## 4. Discussion.

If one keeps the schematic picture of the formation of $Fe_4N$ on the basis of the insertion of N into an f.c.c. lattice of Fe, the main result of the presence of nitrogen would be merely to expand the lattice ($a[Fe_4N] = 3.979$ Å ; $a[\gamma\text{-Fe}] = 3.450$ Å) since at such an expansion f.c.c. Fe is ferromagnetic [17]. Consequently nitrogen can only be held responsible for the lowering of the magnetic moment of Fe(II) by spin pairing. The same assumption can be formulated for Mn. The magnetic characteristics and the shape of the D.O.S. — especially the sharpening effect of Fe(I)'s — can be explained using the « model of covalent magnetism » proposed by Williams *et al.* [18].

The interpretation of the magnetism of a variety of metallic or alloy systems can be correctly provided within the framework of the Stoner model [19, 20]. In this model the magnetic moment results from a rigid-shift in the density of states of an initially paramagnetic system into majority-spin states energetically low-lying and minority-spin states at higher energies. However a shift in spectral weights to majority-spin states below the Fermi energy and minority-spin states above Fermi energy had to be accounted for in order to explain the magnetism of alloys where the Stoner model alone failed to provide a consistent interpretation [18]. Magnetism arising in this way is called « covalent magnetism ».

In $M_4N$ [M = Fe, Mn] the interaction between the states associated with the metal sublattice (II) and N on the one hand and with each one of the two metal sublattices I and II on the other hand can be best seen through a simple correlation diagram of the molecular-orbital-type. It needs to be stressed that for both Fe and Mn at the two lattice sites we start with spin-split levels — due to intra-atomic spin polarization —. The splitting is proportional to the differential occupancy of d sub-bands between up : ↑ and down : ↓ spins and thus to the resulting atomic moment.

As stated formerly, the spin-pairing involves N states and M(II) ones. This leads to the reduction of the atomic moment of M(II) and hence to less-split metal (II) levels with respect to metal (I) ones.

4.1 M(II)-M(I) INTERACTIONS. — Correlation diagrams of the M.O.-type are shown in figure 3a and b for $Fe_4N$ and $Mn_4N$ respectively. In both cases nitrogen valence states are not shown. On the right-hand side of each figure we have represented the D.O.S. for sake of comparison. The construction of the M.O.-type levels shows a redistribution for the relative weights of the bonding and anti-bonding states formed. As can be seen, in the case of $Fe_4N$ (Fig. 3a) the spin-up (↑) state is anti-bonding and the spin-down (↓) state is bonding. Because of the comparable band splitting of the atomic levels these states do not change their energetic positions and the coupling is found to be ferromagnetic. This behaviour is in contrast with that of $Mn_4N$ (Fig. 3b). For this compound we start with one strongly split atomic level Mn(I) ($\mu = -3.2\ \mu_B$) and one much less split atomic level Mn(II) ($\mu = 0.8\ \mu_B$). The interaction between these levels now leads to an interchange of the energetic positions of the spin-up anti-bonding and the spin-down bonding states, so that the latter lies lower in energy. With the Fermi levels determined by the half-filled d-band, this effect leads to a ferrimagnetic coupling between the two Mn sublattices.

4.2 METAL-NITROGEN INTERACTIONS. — In order to check the contribution of t2g and eg components in the 3d metal densities of states to the chemical

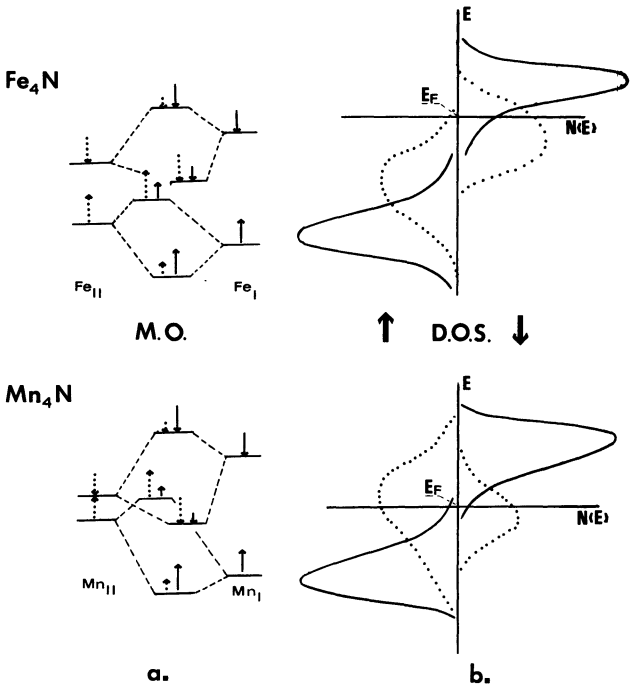


Fig. 3. — Correlation diagrams in the covalent magnetism model for : (a) $Fe_4N$ ; (b) $Mn_4N$.

bond in the nitride, we have calculated the partial D.O.S. for each of the t2g and eg subbands of the metal subblattices. This has been undertaken for $Fe_4N$.

*Hybridization of nitrogen orbitals.* — In the arrangement of the structure given in figure 1a, nitrogen resides at the center of the unit cell. It is surrounded by 6 Fe(II) at $a/2$ and 8 Fe(I) at $a\sqrt{3}/2$. If an sp3 hybridization of N orbitals (2s and 2p) is assumed, then each sp3 lobe would point — axially — towards corner Fe(I) (direction $\langle 111 \rangle$ whereas an indirect (non-$\sigma$) interaction would occur between N and Fe(II)). However, due to Fe $\leftrightarrow$ N distances this hypothesis has to be ruled out. So if N is to have direct bonds with closest metal i.e. Fe(II) then we have to assume an octahedral hybridization of nitrogen orbitals ; i.e. sp3d2. This actually finds support in the plot of the s, p and d-D.O.S. for N (Fig. 4) : the mixing between s and p states can be seen, furthermore the d-D.O.S., although very weak, show an extension towards s and p states. As a consequence direct bonding occurs between N and Fe(II).

a) Nitrogen $\leftrightarrow$ Fe(I) interactions. — Direct N $\leftrightarrow$ Fe(I) interactions are likely to occur along $\langle 111 \rangle$. This leads to an overlap between N(sp3d2) and Fe(I){t2g} — degenerate and hybridized — orbitals in a $\pi$-like manner. Examining the partial d-D.O.S. for Fe(I) shows this tendency (Figs. 5/I for spin-up and 5/III for spin-down directions) : there is no extension of Fe(I){eg} states towards N « p-like » states (between 0 and 0.5 Ryd) whereas t2g states are skewed towards lower energies and there simultaneously appear 3 peaks between 0 and 0.5 Ryd. The intensity of these peaks (hereafter called N1, N2 and N3 with increasing energy) is the following : $I(N1) < I(N2) < I(N3)$. This can be interpreted in terms of : N1 $\equiv$ $\sigma$-like subband, N2 $\equiv$ non-bonding subband and N3 $\equiv$ $\Pi$-like subband. On one hand this is consistent with the type of overlap ($\Pi$-like) between t2g lobes and sp3d2 ones of Fe(I) and N respectively and on the other hand with the discussion of the bonding between Fe(II) and N in next paragraph.

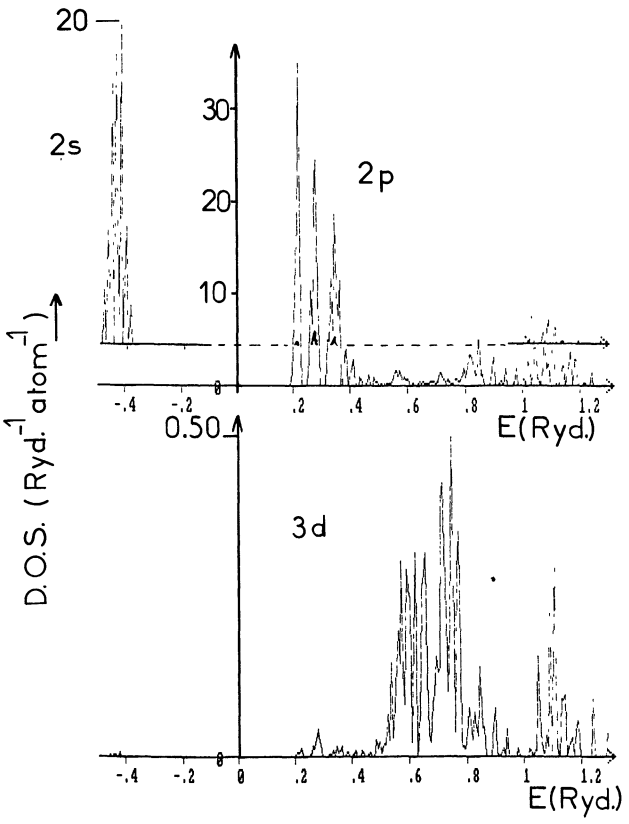


Fig. 4. — $l$-decomposed spin-up D.O.S. for nitrogen in $Fe_4N$.

b) Nitrogen $\leftrightarrow$ Fe(II) interactions. — Fe(II) $\leftrightarrow$ N interactions occur along the $\langle 100 \rangle$ direction and one may expect $\sigma$-like (axial) overlap between Fe(II) and N to occur *via* N(sp3d2) and Fe(II){eg} ; $\Pi$-like overlap through t2g.

Figures 5/II and 5/IV show the partial d-D.O.S. for Fe(II) in both spin directions. One important feature differentiates them from those of Fe(I) : d-bands extend towards s-states of N especially for eg-states ; — actually there is hardly any overlap between Fe(II){t2g} and N{s}-like states —. Inasfar as t2g states of Fe(II) are not degenerate — actually Fe(II) is in a site of D4h point symmetry — the lobes of the dxy orbital would point away from N(sp3d2), therefore no bonding may occur between them. On the other hand it can be seen that the contribution of d-Fe(II) band to N-p-like states (between 0 and 0.5 Ryd) is higher than in Fe(I). This shows the more direct character of the bonding between Fe(II) and N.

In figures 5/II and 5/IV the t2g subbands show between 0 and 0.5 Ryd the following trends : $I(N1) \simeq I(N2) \leqslant I(N3)$. Moreover, for the Fe(II){eg} subband in the same energy region $I(N1) > I(N2) \gg I(N3)$ and an intensity of N1(t2g) < N1(eg) can be observed : this can be interpreted in terms of maximum $\Pi$-bonding between N(sp3d2) and Fe(I){t2g}-like orbitals and maximum $\sigma$-like bonding between N(sp3d2) $\leftrightarrow$ Fe(II){eg}.

It needs to be stressed that this approach — i.e. M.O. description — is a « low limit » one because $Fe_4N$ has metallic behaviour : $\rho$ ($\mu\Omega$ cm) at 25 °C $\simeq$ 10 000. In other words the decomposition of d-states into the octahedral crystal-field components is only a scheme to improve our understanding. The success of this scheme is necessarily limited by the mixing of orbitals not only within t2g and eg respectively but between them as well (t2g and eg subbands occur in the same energy range : from 0.5 to $\simeq$ 0.85 Ryd).

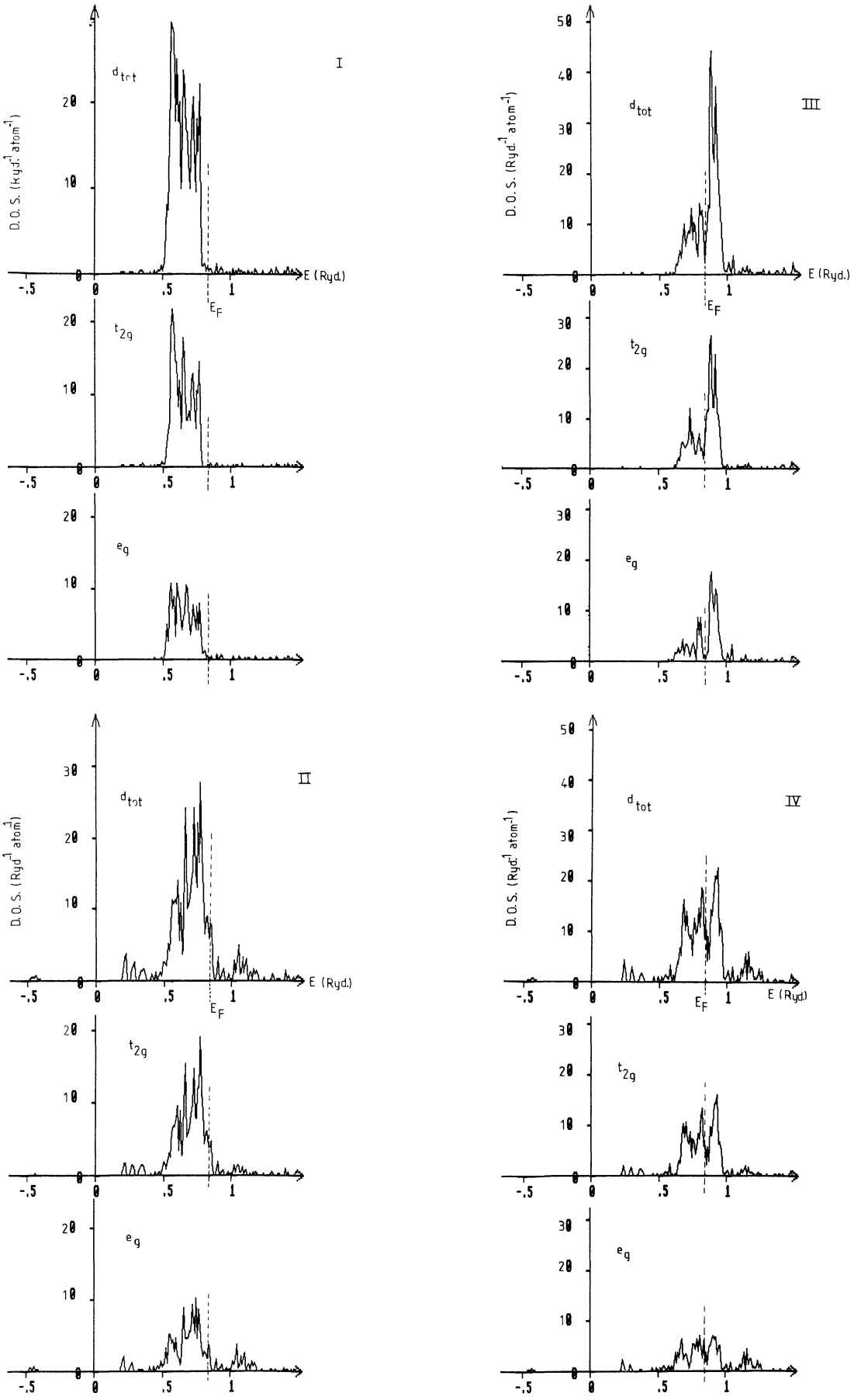


Fig. 5. — Partial site projected d-D.O.S. for : I — Fe(I) spin-up ; II — Fe(II) spin-up ; III — Fe(I) spin-down ; IV — Fe(II) spin-down.

## 5. The hyperfine fields in $Fe_4N$ and $Mn_4N$.

The effective magnetic field $H_{eff}$ acting on a nucleus is usually written as the sum of 4 contributions :

$$H_{eff} = H_i + H_{FC} + H_{orb.} + H_{dip.}$$

$H_i$, the internal field, is the magnetic field at the nucleus generated from an externally applied field.

$H_{FC}$ is the Fermi-contact term — or hyperfine interaction — arising from an unbalanced spin-density of the s-electrons at the nucleus (in a non-relativistic description) :

$$H_{FC} = -\frac{8\pi}{3}\gamma_N\{(\Phi_\uparrow(0))^2 - (\Phi_\downarrow(0))^2\}$$

where $\gamma_N$ is the nuclear gyromagnetic ratio and the quantities between brackets are the densities of the s-electrons at the nucleus ($r = 0$) for spin up and spin down respectively.

$H_{orb.} + H_{dip.}$ are the fields arising from the orbital magnetic moment (small for 3d-metals) and from the dipole interaction with the surrounding atoms ($H_{dip.}$ is zero for cubic symmetry).

Table II gives our calculated values of Fermi-contact hyperfine fields for the metal and nitrogen sites. A comparison with experimental values obtained from Mössbauer results for $Fe_4N$ shows a good agreement [21].

Table II. — *Calculated values of Fermi-contact hyperfine field compared to available experimental data.*

| | | Atomic Moment | $H_{FC}$ (kG) | Experiment $H$ |
|---|---|---|---|---|
| $Fe_4N$ | Fe(I) | 2.98 | − 299.90 | − 340 (*) |
| | Fe(II) | 1.79 | − 204.40 | − 217 (*) |
| | N | 0.02 | − 12.48 | |
| $Mn_4N$ | Mn(I) | − 3.23 | 51.55 | |
| | Mn(II) | 0.80 | − 32.28 | |
| | N | − 0.07 | − 35.24 | |

(*) D. Andriamandroso *et al.* [21].

## 6. Comparison with the phenomenological model.

A schematic energy-band representation for $Fe_4N$ — as well as for other metal : non-metal compounds — is given in a review article on perovskite-type compounds by Goodenough and Longo [22]. A sketch of the energy-band scheme in conjunction with the calculated D.O.S. for $Fe_4N$ is shown in figure 6. There is a close qualitative agreement between both schemes with respect to the proposed spin alignments and to the distribution of the localized states at the bottom and top of the bands.

## 7. Comparison with Heusler alloys.

Kübler *et al.* [23] describe the formation and coupling of magnetic moments in Heusler alloys. These alloys are systems of the type $X_2MnZ$ where the X-atoms (e.g. Cu, Pd) serve primarily to determine the lattice constant while the Z-atoms (e.g. Al, In, Sb) mediate the interaction between the Mn d-states. The Mn atoms, which carry a magnetic moment, form exactly the perovskite-type sublattice as found in our system. The atom at the center of the cubic cell also provides only p-states — Al, etc. — in the

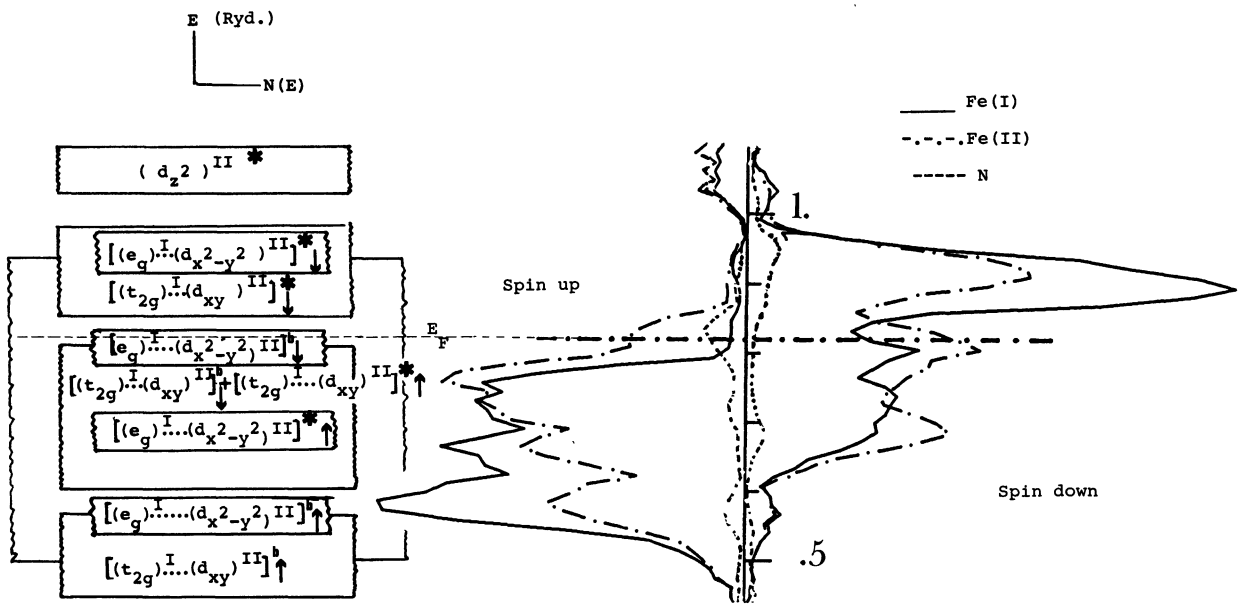


Fig. 6. — Comparison of the calculated D.O.S. of $Fe_4N$ with Goodenough's diagram of the electronic structure of $Fe_4N$.

Heusler lattice, nitrogen in our case. The transformation from Heusler to $M_4N$-type structure (M = Mn, Fe) can be achieved by removing the non-magnetic X atoms and three out of the four atoms found in the cubic cell, thus making the Mn, Fe positions non-equivalent. To provide for the necessary interactions we replace these 3 Z atoms by empty spheres (pseudo-atoms) as stated above.

Kübler *et al.* [23] find antiferromagnetic ordering of the Mn atoms with magnetic moments between 2.74 and 3.90 $\mu_B$ per Mn, depending on the compound, which is in the same range as the 3.23 $\mu_B$/Mn(I) calculated for $Mn_4N$. Because of the non-equivalency of the Mn positions in $Mn_4N$ we find only ferri-magnetic magnetic ordering, instead of antiferromagnetic alignment in the Heusler alloys.

The missing Z atoms, which in the Heusler alloy provide a mediating p-d interaction between the Mn atoms, lead to a similar localization of the magnetic moments on Mn(I) but for a slightly different reason. Whereas in the Heusler alloy the spin-up states do not form a common band with their neighbouring atoms (in contrary to the spin down states) and thus appear to be excluded leading to a localization of the Mn moment, in $Mn_4N$ a different mechanism is found. The large lattice constant leads to an isolation of the corner sites. These atoms show an almost free-atom-like electronic configuration. The interaction with the neighbouring M(II) sites are weak and lead only to a minor hybridization of the d-states along these symmetry directions.

The non-interacting remaining d-states thus split completely according to Hund's rules forming these very pronounced peaks in the density of states (Fig. 2b).

## 8. Conclusions.

In this study it has been shown that the A.S.W. method is quite adapted for the calculation of the electronic and magnetic characteristics of transition metal nitrides of the $M_4N$ perovskite-type structure.

The calculated magnetic structures of $Fe_4N$ and $Mn_4N$ (ferro- and ferri-magnetic respectively) are in agreement with literature and the values for the atomic moments are close to experimental ones.

The electronic structures calculated for both materials rule out any ionic character in such nitrides and the density of states — at least for $Fe_4N$ — compare fairly well with the existing schematic electronic structure proposed in literature.

## Acknowledgments.

The authors wish to express their gratitude to the late Professor E. P. Wohlfarth of the Imperial College of Science and Technology — London, U.K. — for critical discussions and for his supporting interest in this work. One of us (S. M.) wishes to acknowledge support from the computer center of the University of Bordeaux (C.I.C.BX.).

## References

[1] SUZUKI, S., SAKUMOTO, H., MINEGISMI, J. and OMOTE, Y., *I.E.E.E. Trans. Magn.* **MAG17** (1981) 3017.

[2] TAGAWA, K., KITA, E. and TASAKI, A., *J. Phys. Soc.* **21** (1982) 1596.

[3] DEMAZEAU, G., ANDRIAMANDROSO, D., POUCHARD, M., TANGUY, B. and HAGENMULLER, P., *C. R. Hebd. Séan. Acad. Sci. II* **297** (1983) 843.

[4] FRAZER, B. C., *Phys. Rev.* **112** (1958) 751.

[5] WIENER, G. W. and BERGER, J. A., *J. Met.* **7** (1955) 360.

[6] GOODENOUGH, J. B., WOLD, A. and ARNOTT, R. J., *J. Appl. Phys.* **31** (1960) 342S.

[7] ELLIOTT, W., *Phys. Rev.* **129** (1963) 1120.

[8] ANDRIAMANDROSO, D., DEMAZEAU, G., POUCHARD, M. and HAGENMULLER, P., *J. Solid State Chem.* **54** (1984) 54.

[9] FRUCHART, D., GIVORD, D., CONVERT, P., L'HÉRITIER, P. and SÉNATEUR, J. P., *J. Phys. F.* **9** (1979) 2431.

[10] WILLIAMS, A. R., KÜBLER, J. and GELATT, C. D. Jr., *Phys. Rev. B* **19** (1979) 6094.

[11] VON BARTH, J. and HEDIN, D., *J. Phys. C* **5** (1972) 1629.

[12] JANAK, J. F., *Solid State Commun.* **25** (1978) 53.

[13] SCHWARZ, K., MOHN, P., BLAHA, P. and KÜBLER, J., *J. Phys. F.* **14** (1984) 2659.

[14] ROMPA, H. W. A. M., SCHUURMANS, M. F. H. and WILLIAMS, F., *Phys. Rev. Lett.* **52** (1984) 675.

[15] SCHWARZ, K., *J. Phys. F* **16** (1986) L211.

[16] ZENER, C., *Phys. Rev.* **85** (1952) 324.

[17] MORUZZI, V. L., MARCUS, P. M., SCHWARZ, K. and MOHN, P., *Phys. Rev. B* **34** (1986) 1784.

[18] WILLIAMS, A. R., ZELLER, R., MORUZZI, V. L., GELATT, C. D. Jr. and KÜBLER, J., *J. Appl. Phys.* **52** (1981) 2067.

[19] HERRING, C., Magnetism, Vol. IV, Eds. G. T. Rado and H. Suhl (Academic Press, N.Y.) (1966) 256.

[20] WOHLFARTH, E. P., *J. Magn. Magn. Mat.* **45** (1984) 1.

[21] ANDRIAMANDROSO, D., FEFILIATIEV, L., DEMAZEAU, G., FOURNÈS, L. and POUCHARD, M., *Mat. Res. Bull.* **19** (1984) 1187.

[22] GOODENOUGH, J. B. and LONGO, D., Landolt-Börnstein, Neue Serie III/4a (Berlin) 1970.

[23] KÜBLER, J., WILLIAMS, A. R. and SOMMERS, C. B., *Phys. Rev. B* **28** (1983) 1745.

[24] TAKEI, W. J., HEIKES, R. R. and SHIRANE, G., *Phys. Rev.* **125** (1962) 1893.